J. Fluid Mech. (1974), *vol.* 65, *part* 3, *pp.* 439–459
Printed in Great Britain

The structure of the viscous sublayer and the adjacent wall region in a turbulent channel flow

By HELMUT ECKELMANN

Max-Planck-Institut für Strömungsforschung, Göttingen, West Germany

(Received 2 April 1973 and in revised form 21 January 1974)

Hot-film anemometer measurements have been carried out in a fully developed turbulent channel flow. An oil channel with a thick viscous sublayer was used, which permitted measurements very close to the wall. In the viscous sublayer between $y^+ \simeq 0{\cdot}1$ and $y^+ = 5$, the streamwise velocity fluctuations decreased at a higher rate than the mean velocity; in the region $y^+ \lesssim 0{\cdot}1$, these fluctuations vanished at the same rate as the mean velocity.

The streamwise velocity fluctuations u observed in the viscous sublayer and the fluctuations $(\partial u/\partial y)_0$ of the gradient at the wall were almost identical in form, but the fluctuations of the gradient at the wall were found to lag behind the velocity fluctuations with a lag time proportional to the distance from the wall. Probability density distributions of the streamwise velocity fluctuations were measured. Furthermore, measurements of the skewness and flatness factors made by Kreplin (1973) in the same flow channel are discussed. Measurements of the normal velocity fluctuations v at the wall and of the instantaneous Reynolds stress $-\rho uv$ were also made. Periods of quiescence in the $-\rho uv$ signal were observed in the viscous sublayer as well as very active periods where ratios of peak to mean values as high as 30:1 occurred.

1. Introduction

Hot-wire measurements of the fluctuating velocities u and v in the streamwise direction and normal to the wall, respectively, in a fully developed turbulent channel flow were first published by Reichardt (1938). In 1950 Laufer published measurements, also obtained with hot-wire probes in a fully developed turbulent channel flow, which largely confirmed Reichardt's results and extended the v-component results to distances closer to the wall. In addition, Laufer also measured the component w parallel to the wall.

In order to facilitate further measurements in turbulent channel flows in the region where viscosity plays the major role, in 1953 Reichardt developed a flow channel in which a viscous sublayer approximately 1 cm thick can be obtained by using oil as the fluid and maximum velocities of approximately 20 cm/s. In air or water, the fluids normally used for laboratory experiments, the thickness of the viscous sublayer lies between approximately 0·1 and 1 mm at the velocities most commonly used. By using glycerin for his experiments, Bakewell (1966) has also obtained a thick viscous sublayer.

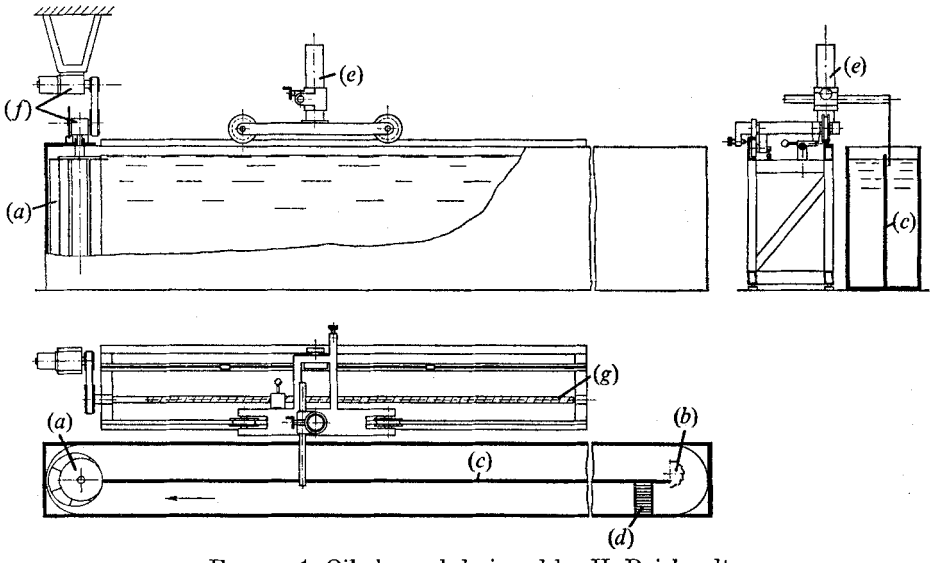

FIGURE 1. Oil channel designed by H. Reichardt.

When the oil channel was put into operation in 1954 attempts at making quantitative measurements were unsuccessful because the hot-wire probes used did not perform adequately in the oil. The channel was therefore used only for demonstration purposes. In 1969, after quartz-coated hot-film probes had been developed and become commercially available, quantitative measurements in the oil channel became possible, and the measurements of the turbulent velocity components u and v and of their product uv reported here were begun.

2. Experimental facility

The channel consists of an open steel tank (figure 1) 8·5 m long, 0·5 m wide and 1 m deep, which is filled with oil to a depth of 0·85 m. At one end of the tank stands a pump (*a*); at the other end, turning vanes (*b*) are mounted. The space between the pump and the turning vanes is divided into two regions, nearly equal in size, by a wooden partition (*c*) running the length of the channel. When the pump is in operation, the oil flows down the channel to the turning vanes on one side and returns to the pump on the other side. The return-flow region is the actual channel flow used for the measurements reported here. The observations and measurements were carried out near the inlet of the pump. This area is about 7 m downstream from the turning vanes, and here the wooden partition is coated with plastic. The channel is 22 cm wide and 32 channel widths long. Experience has shown that fully developed channel flow can be obtained within this length, provided that the flow velocity in the channel entrance is relatively uniform and the flow is tripped. These conditions were met by installing a honeycomb and a fine mesh screen (*d*) just downstream of the turning vanes. Both vertical sides of the screen frame are sharp, and thus act as the tripping device. It will be shown in §4 that 32 channel widths are sufficient to produce a fully developed turbulent flow.

To fill the channel, 3·6 m^3 of oil are needed. Shell oil 3101, pure paraffin-based and normally refined without additives, was chosen for the experiments. It has a kinematic viscosity ν of 6×10^{-2} cm^2/s at 25 °C, which is 6 times that of water and 0·4 times that of air. At the maximum centre-line velocity attainable in the channel, approximately $\overline{U}_c = 22{\cdot}5$ cm/s, the Reynolds number is $Re_U = \overline{U}_c b/\nu = 8200$, where b is the channel width. The smallest Reynolds number at which the flow in the oil channel remains fully turbulent is $Re_U = 5600$. At these Reynolds numbers, a distance of 1 cm from the wall corresponds to $y^+ = 19$ and $y^+ = 13$ respectively. The maximum sublayer thickness in this channel is 1·4 times that which Bakewell (1966) achieved in his investigations. The equivalent pipe Reynolds numbers based on the hydraulic diameter are about 15000 and 10000 respectively.

In order to make hot-film measurements in oil possible, it is necessary to remove all solid elements, including the resin particles formed by oxidation of the oil. This was achieved by using two filters from Millipore, types CP 13022 and CTAA 022, arranged one behind the other. Such filters trap all particles larger than 0·8 μm. The oil was pumped through the filter installation twice before it was placed in the channel. The degree of purity reached was sufficient for all the measurements, which were taken over a period of more than one year. The channel is kept closed to prevent dust contamination and is uncovered only as much as necessary during measurement and calibration.

Quantitative measurements require that the temperature of the oil does not vary with time and position. To meet this requirement, the temperature in the room where the channel is located is kept constant at 25 °C by means of electric heaters distributed in the room and controlled by contact thermometers. Under these conditions, the temperature of the flowing oil is $24{\cdot}5 \pm 0{\cdot}1$ °C. The channel pump is driven by a three-phase a.c. motor with a variable gear system (f) at a revolution rate which is constant to within 0·05 %.

Adjacent to the channel, a probe support is mounted on a carriage (e) which can be moved with variable velocity parallel to the channel wall over a distance of 2·8 m by means of a driving spindle (g). The velocity of the carriage can be adjusted within the range of speeds 0·2–23 cm/s and is measured electrically. This arrangement permits calibration of the probes directly in the flow facility used for the measurements.

The velocity measurements were made with quartz-coated hot-film probes, type 1210–20W (single probe) and type 1241-20W (X-probe), manufactured by Thermo-Systems, Inc. For the gradient measurements at the wall, a quartz-coated hot-film wall element from DISA, type 55A91, was used. Quartz-coated probes had to be used because the oil interacts with platinum or platinum-alloy probe surfaces. The various effects observed with hot-wire probes and uncoated hot-film probes in oil flow have been reported by the author (1972) elsewhere. Constant-temperature anemometers and linearizers from DISA were also used.

An analog computer was constructed and used to make true-mean, mean-square and correlation measurements. It consisted of three Burr–Brown multipliers and three integrating digital voltmeters with one time base and with integration times up to 60 s. Owing to the very low frequencies of the measured

fluctuating quantities in this flow, very long run times were necessary. To obtain time-independent mean values, 20 min and 10 min samples were taken for the low and high Reynolds numbers, respectively. Two Krohn–Hite filters were used to suppress the d.c. component corresponding to the local mean streamwise flow velocity $\overline{U}$ and to filter out the frequencies outside the range of the turbulent fluctuations (50 Hz hum and noise). The latter was especially important, since the hot-film signals were very weak because of the small overheat ratio of the probes used. Every precaution was taken to minimize errors in the analog circuit due to d.c. bias, variable gain, etc. This was done by testing the circuit system with fixed d.c. voltages and sine waves before processing the turbulent signals. The time functions of the fluctuating signals were obtained with a liquid-beam oscillograph (Siemens Oszillomink), and the probability density distributions with a LABEN multichannel analyser. More details of the facility can be found in Eckelmann (1970).

3. Calibration of the anemometry system of the probes and tests

As mentioned, the oil channel has the advantage that both measurements and calibration can be performed without moving the probes to a separate calibration facility. The probes are mounted on the calibration carriage (*e*) (see figure 1); they can be moved with the help of a driving spindle as described above. During measurement, the calibration carriage is locked in place. For calibration, however, with no flow in the channel, the carriage is released and a motor drives the spindle, which in turn drives the carriage forward with a constant velocity and no slip. The velocity is automatically measured, and the carriage disengages itself at the end of the spindle. It was unnecessary to alter the electronics of the experimental apparatus for the calibration, so that calibration and measurement conditions were identical.

For all measurements, the temperature difference between the oil and the hot-film probe was approximately 5 °C, corresponding to an overheat ratio R_w/R_k of 1·01. This temperature difference was chosen in order to ensure that the convection produced by the hot film itself would remain as small as possible, and so that the frequency response of the hot film would still be sufficiently high.

The influence of the convection is indicated by a bend in the linearized calibration curve at very low velocities. This bend limits the linear velocity range of the anemometer system at the lower end. For these measurements, this lower limit could be reduced to 0·5 cm/s, so that reliable measurements down to wall distances of $y^+ \gtrsim 0{\cdot}8$ were made possible.

Since the temperature of the entire laboratory was controlled, the electronic equipment, which was left on during the entire measurement period, was also kept at a constant temperature, so that very little drift occurred. The calibration curves, which were checked before and after each series of measurements, could almost always be reproduced; when they were not reproduced, the measurements were repeated.

Apart from Bakewell's (1966) measurements, carried out with similar probes in glycerin at a Prandtl number of approximately 2000, no information on the

frequency response of hot-film probes in oil was available. The frequency response was therefore estimated by the square-wave method. With the oil used here, $Pr = 82$, which yields a ratio of the thicknesses of the thermal and viscous boundary layers of $\delta_T/\delta \approx \frac{1}{9}$. The equation given by Freymuth (1967), $f_g = 1/1{\cdot}5t_g$ (where t_g is the time from the beginning of the square-wave pulse until the pulse has dropped to 3 % of its maximum value), was used to determine the upper frequency limits for several conditions. In order to make these measurements possible, the square-wave generator built into the anemometer, whose frequency is too high, was disconnected and a square-wave of frequency of 10 Hz was fed into the anemometer from an outside source. For the overheat ratio of 1·01 used here, and for a probe located at the channel centre-line, the upper frequency limit is $f_g = 650$ Hz; for $y^+ \approx 3{\cdot}5$, $f_g = 525$ Hz. With no flow in the channel, $f_g = 57$ Hz. The channel operates at very low velocities, and the upper frequency limit of the turbulence signals at the centre-line lies well below 20 Hz. Therefore, no high frequency response is lost when the probe is operating at this low temperature difference.

When a hot-film probe is operated at a low overheat ratio, it becomes sensitive to temperature as well as velocity fluctuations, which cannot be distinguished from one another. Temperature fluctuations in the frequency range of the turbulence could possibly originate at the positive displacement pump. From an estimate of the energy dissipation in the region between the pump blades and the wall, one can calculate that a localized hot region with a temperature of the order of 2×10^{-3} °C above the steady-state temperature in the flow could be created, and that this would have to travel 16 m in about 80 s (with the centre-line velocity) to get to the test section. Unsteady heat-transfer calculations indicate that the possible temperature increase at the probe due to this hot region would be negligible. A corresponding estimate of the temperature increase caused by dissipating eddies is $0{\cdot}8 \times 10^{-3}$ °C. For this estimate, the maximum shear rate was assumed to be $40\,\mathrm{s}^{-1}$ (cf. figure 4).

Three direct tests were also performed to verify that there were no significant temperature fluctuations. First, the centre-line velocity of the turbulent flow was reduced to 4·5 cm/s, which gave laminar flow. The fluctuations in the anemometer output signals decayed in 85 s. If temperature fluctuations existed, they should have persisted for several hundred seconds at a lower frequency and with an amplitude only slightly diminishing with time. In the second test, an anemometer was operated as a resistance thermometer, and no fluctuations in temperature could be detected. Finally, at an early stage in these investigations, measurements were carried out with an overheat ratio of 1·2, corresponding to a temperature difference of 100 °C between the oil and hot film, at wall distances where convection currents produced by the hot film itself could be neglected. These measurements completely reproduced the later ones taken with the lower overheat ratio of 1·01. Thus, it can be concluded that temperature fluctuation effects are negligible.

The measurement of the velocity gradient at the wall made calibration and testing of the hot-film wall element also necessary. The sensitive platinum foil, 1 mm long and 0·2 mm wide, was placed with its long axis normal to the stream-

wise direction. The hot-film wall element was operated exactly like the hot-film probe but with an overheat ratio of 1·02, which corresponds to a temperature of the foil about 8 °C above that of the flowing oil. The upper frequency limit of the wall element determined by the square-wave method is $f_g = 250\,\mathrm{Hz}$; it remains the same whether there is flow or not. The calibration curve for the hot-film wall element was derived from averaged velocity gradients at the wall for different centre-line velocities. These gradients were measured with the hot-film probe and related to the corresponding average output voltages of the wall element.

At this point, additional possible errors in hot-wire and hot-film measurements at high turbulence intensities must be considered. For a single-film probe positioned parallel to the wall and normal to the flow, Bakewell (1966) has made a fourth-order estimate of the combined error in measuring the u component due to the additional sensitivity of the hot film to the other component v normal to the film and to his nonlinearized signal. This can be taken as an estimate of the error in the present measurements, although linearized signals were used here. He obtained a constant error of about 7 % for $y^+ \lesssim 10$. For larger y^+ values, the error becomes significantly smaller.

An estimate of the error in u-component measurements with a single-film probe positioned normal to the wall and the flow due to w fluctuations, which are also normal to the probe, can be made from the work of Klatt (1973). Using a third-order approximation, he shows that

$$\left(\frac{\overline{u^2}}{\overline{U}^2}\right)_{\mathrm{true}} = \left(\frac{\overline{u^2}}{\overline{U}^2}\right)_{\mathrm{meas}} \left\{1 + \frac{1}{(\overline{u^2}/\overline{U}^2)_{\mathrm{meas}}} \left[a^2 \frac{\overline{uv}}{\overline{U}^2} + 2k\left(\frac{\overline{u^2}}{\overline{U}^2} - \frac{k}{4}\frac{\overline{w^2}}{\overline{U}^2}\right)\frac{\overline{w^2}}{\overline{U}^2}\right]\right\},$$

where a and k are empirical constants. Using Laufer's (1954) measurements, and taking $a = 0$ and $k = 1{\cdot}4$, there is a maximum error of 5 % at $y^+ = 1$. This decreases to about 2·5 % at $y^+ = 3$, agreeing fairly well with Bakewell's estimate. To translate these results to an X-probe mounted in the x, y plane with both films at 45° to the flow, one must assume that the w fluctuations do not produce a wake from one film on the other, and that the effect of w fluctuations on a single film mounted normal to the flow and the wall is not very different from the effect when the film is mounted at 45° to the flow. The v velocity is obtained from the difference in the two film signals, in which case the errors due to the w fluctuations cancel. For the u velocity, these errors are additive. In other words one must add $2w$ to $2 \times 0{\cdot}707(\overline{U} + u)$ to obtain the total velocity vector normal to the film and the maximum error should be about $2w/1{\cdot}414\overline{U} \approx (2 \times 1{\cdot}025\overline{U})/1{\cdot}414\overline{U} = 3{\cdot}5\,\%$. This error decreases with increasing y^+.

The error due to the influence of the wall on the heat transfer from the hot film was tested with no flow by systematically bringing the probe closer to the wall. Up to distances $y^+ \approx 0{\cdot}6$ ($y = 0{\cdot}3\,\mathrm{mm}$), no change in the linearized anemometer output could be detected, so that the influence of the wall can be neglected for the measuring positions $y^+ > 0{\cdot}8$ of this work.

4. The flow conditions in the oil channel

The region chosen for the measurements in the flow channel lies 675 cm downstream from the screen and 10 cm below the surface of the oil. In order to show that the turbulent flow is fully developed at the measuring station, the skewness and flatness factors $\overline{u^3}/(\overline{u^2})^{\frac{3}{2}}$ and $\overline{u^4}/(\overline{u^2})^2$ of the streamwise fluctuations were measured for both Reynolds numbers along the centre-line at this station and at one and two channel widths upstream. As Comte-Bellot (1965) has shown, both factors, in the central region, are strongly dependent on the degree to which the turbulent channel flow is developed. First, several runs were made at the measuring station. The flow was switched off and the probe was moved and then repositioned at the centre-line between each run. With this procedure,

$$\overline{u^3}/(\overline{u^2})^{\frac{3}{2}} = 0{\cdot}57 \pm 3\,\% \quad \text{and} \quad \overline{u^4}/(\overline{u^2})^2 = 3{\cdot}51 \pm 0{\cdot}8\,\%.$$

When the probe was not moved between measurements, the reproducibility was considerably better. At one channel width upstream, the skewness and flatness factors agreed with the above values to within 3·1 % for $\overline{u^3}/(\overline{u^2})^{\frac{3}{2}}$ and 0·7 % for $\overline{u^4}/(\overline{u^2})^2$. At two channel widths upstream, the corresponding values agreed to within 2·3 % and 0·8 %. Measurements of the skewness and flatness factors of the fluctuating component normal to the wall at the measuring station gave $\overline{v^3}/(\overline{v^2})^{\frac{3}{2}} = 0$ and $\overline{v^4}/(\overline{v^2})^2 = 3{\cdot}6 \pm 1{\cdot}3\,\%$. The variation of these values with upstream distance was about the same as that for the streamwise fluctuations. As can be seen, these values do not change, within the measurement accuracy, over two channel widths upstream of the normal measuring station. It can thus be concluded that the flow in the channel is fully developed.

Figures 2 and 3 show the distribution of the local mean velocity for both Reynolds numbers across the channel plotted non-dimensionally. It can be seen that the flow is symmetrical and that the law of the wall holds for both Reynolds numbers. Additional measurements (not presented here) showed that the velocity profile was entirely independent of position and thus demonstrated that the present measurements are free of surface and channel-bottom influences.

The hot-film wall element was flush mounted into the central partition of the channel 675 cm downstream from the screen and 10 cm below the surface. Figure 4 shows records of the time-varying gradient at the wall obtained with the wall element for the Reynolds numbers 5600, 6800 and 8200. As can be seen, the wall gradient is always positive. The thermal inertia of the hot-film wall element, in the constant-temperature mode, can be completely ignored under the present operating conditions (frequencies far under 20 Hz at the wall; cf. Bakewell 1966, figure 34), since the upper frequency limit of this element was found by the square-wave method to be 250 Hz. It can be stated with certainty, therefore, that there are no negative velocities near the wall. In all three cases, the velocity gradient fluctuates within the range approximately 0·4–1·7 times the mean. A continuously positive velocity gradient at the wall was also observed by Popovich & Hummel (1967), using photographic means to make the gradients at the wall visible.

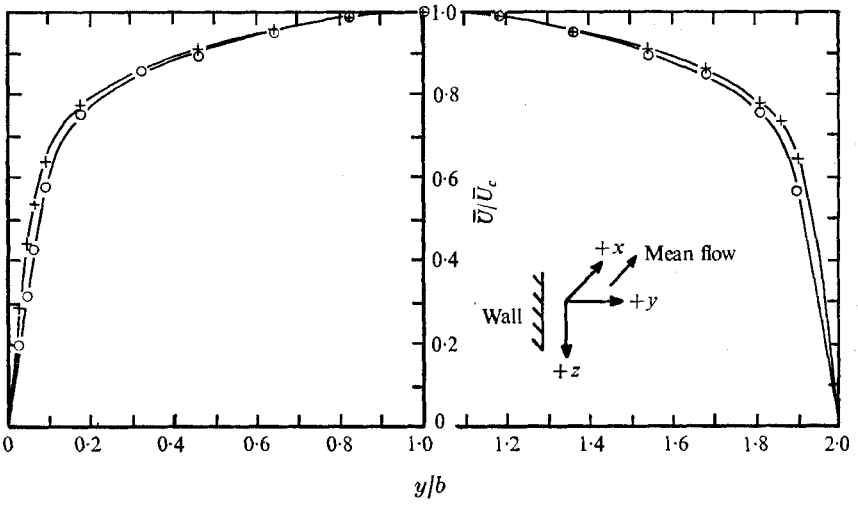

FIGURE 2. Distribution of the local mean velocity across the channel width. ○, $Re_U = 5600$; +, $Re_U = 8200$.

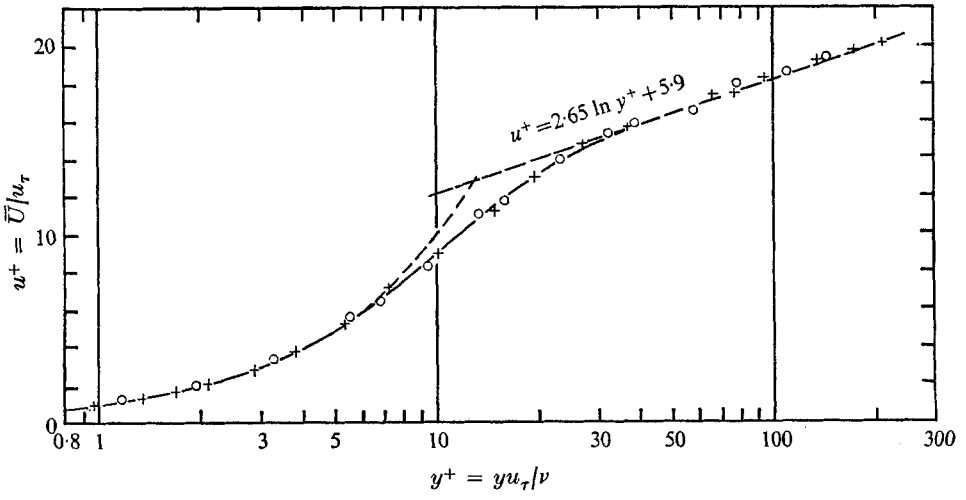

FIGURE 3. Distribution of the local mean velocity in non-dimensional co-ordinates, ○, $Re_U = 5600$; +, $Re_U = 8200$.

5. New effects observed in the wall region

5.1. *The streamwise velocity fluctuations*

The r.m.s. values of the streamwise velocity fluctuations u non-dimensionalized with the friction velocity $u_\tau = (\tau_0/\rho)^{\frac{1}{2}}$ are shown in figure 5 as a function of the non-dimensional wall distance y^+ for Reynolds numbers 5600 and 8200 (in this paper, a prime denotes a root-mean-square value). In this figure, the points for both Reynolds numbers collapse onto one curve. The maximum of the curve lies at approximately $y^+ = 13$, where the viscous and turbulent shear stresses are equal. The maximum value of u'/u_τ measured is approximately 2·8 and differs

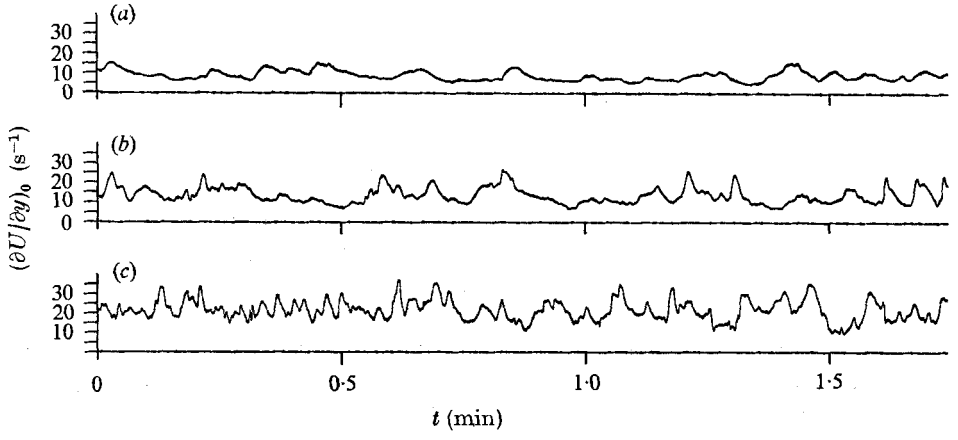

FIGURE 4. Velocity gradient at the wall as a function of time. (*a*) $(\partial\overline{U}/\partial y)_0 = 10\ \mathrm{s}^{-1}$, $Re_U = 5600$. (*b*) $(\partial\overline{U}/\partial y)_0 = 15{\cdot}5\ \mathrm{s}^{-1}$, $Re_U = 6800$. (*c*) $(\partial\overline{U}/\partial y)_0 = 21{\cdot}7\ \mathrm{s}^{-1}$, $Re_U = 8200$.

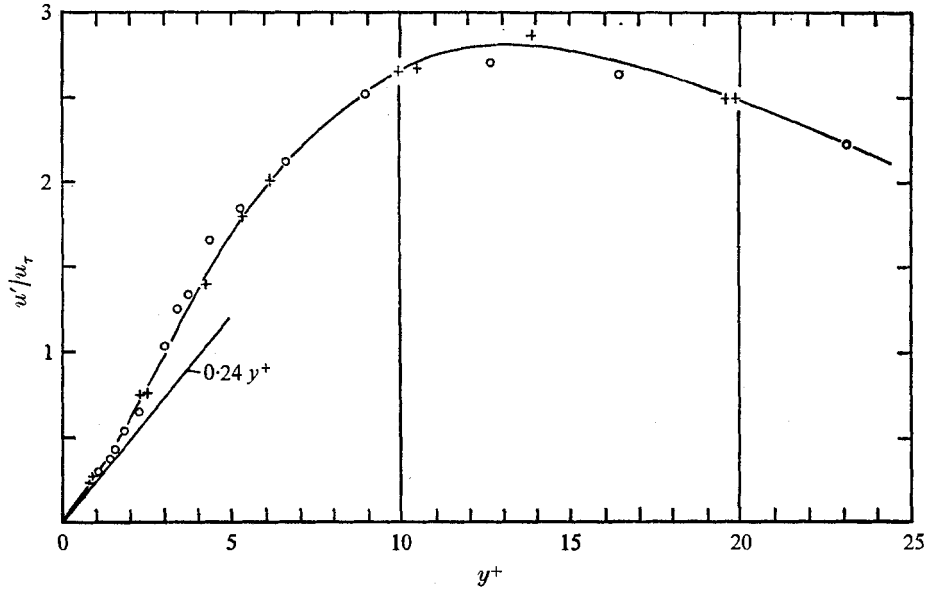

FIGURE 5. Distribution of the r.m.s. values of the streamwise velocity fluctuations in the vicinity of the wall normalized with the friction velocity. ○, $Re_U = 5600$; +, $Re_U = 8200$.

only slightly from the maximum value of 2·6 which Bakewell (1966) found for $Re = 8700$ at $y^+ = 13$. Here, measurements in the region between $y^+ = 5$ and the wall have been made at very small y^+ intervals. As mentioned earlier, no reliable measurement closer than $y^+ \approx 0{\cdot}8$ could be taken with the hot-film probe, however. The shape of the curve indicates that for $y^+ \lesssim 4$ the streamwise fluctuations decrease at a higher than linear rate as the wall distance decreases.

The behaviour of the streamwise fluctuations very near the wall can be determined from the measurements made with the flush-mounted hot-film wall element. The linearized output voltage E of the hot-film wall element is proportional to the velocity gradient at the wall:

$$E = k(\partial U/\partial y)_0.$$

Since $U = \bar{U} + u$, the output voltage consists of a mean $\bar{E}$ and a fluctuating component e:

$$E = k(\partial \bar{U}/\partial y)_0, \quad e = k(\partial u/\partial y)_0.$$

Assuming that, at very small distances from the wall, the instantaneous flow velocity is proportional to the distance from the wall, it follows that

$$\bar{E} = k\left(\frac{\partial \bar{U}}{\partial y}\right)_0 = k\left(\frac{\bar{U}}{y}\right)_0, \quad e = k\left(\frac{\partial u}{\partial y}\right)_0 = k\left(\frac{u}{y}\right)_0$$

and thus

$$e'/\bar{E} = (u'/\bar{U})_0 = a.$$

The ratio $(u'/\bar{U})_0$ at the wall, which is designated here as a, can therefore be measured with the hot-film wall element. The value of a obtained with this device is approximately 0·24 for both Reynolds numbers. Since in the immediate vicinity of the wall $y^+ = u^+ = \bar{U}/u_\tau$, it follows from the definition $(u'/\bar{U})_0 = a$ that $u'/u_\tau \to ay^+$ as the wall is approached. The straight line $u'/u_\tau = ay^+$ is plotted in figure 5. The measured values approach this line asymptotically with decreasing distance from the wall. The fact that this asymptotic slope a of the curve in the immediate vicinity of the wall is non-zero and that the streamwise fluctuations u' decay with wall distance at a higher than linear rate for

$$0{\cdot}1 \lesssim y^+ \lesssim 4$$

suggests that a viscous wall layer $0 \leqslant y^+ \lesssim 0{\cdot}1$ exists under the viscous sublayer. In this wall layer, the streamwise fluctuations u' and the mean velocity $\bar{U}$ both vanish linearly with decreasing wall distance; whereas for the rest of the viscous sublayer $0{\cdot}1 \lesssim y^+ \lesssim 5$, this only holds for the mean velocity $\bar{U}$. Therefore, the supposition mentioned above, that the instantaneous streamwise velocity very near the wall is proportional to the distance from the wall, seems justified.

Recently, Kreplin (1973) was able to reproduce these measurements with the oil channel fitted with a top cover to eliminate possible surface influences. His measurements were taken at the same x co-ordinate as the measurements reported here, but halfway between the bottom and the top of the channel, which is outside both of the boundary layers.

Fortuna & Hanratty (1971) and Py (1973) have also measured the constant a with electrochemical devices. These devices measure the mean shear stress at the wall and both obtained a value of $a = 0{\cdot}3$. An estimate of the wall value $a \approx 0{\cdot}3$ can also be obtained from Bakewell's (1966) measurements. The straight line $u'/u_\tau = 0{\cdot}24y^+$ obtained here and shown in figure 5, on the other hand, agrees with the asymptotic slope of Laufer's (1950) measured values near the wall rather well.

Reichardt (1971) made an attempt to describe the nonlinear behaviour of u' with increasing wall distance. Neglecting the convection terms in the equation of motion and introducing the boundary-layer hypothesis, he was able to show that fluctuations of the viscous shear stress $\tau = \mu \partial u/\partial y$ in the viscous sublayer $y^+ < 5$ are governed by a differential equation of the heat-conduction type. The solution of this equation yields

$$u'/u_\tau = 0{\cdot}24y^+ e^{\frac{1}{2}ay^+},$$

where α is a constant. Obermeier (1972) also analysed the data presented here and found that the decrease in the streamwise fluctuations u' with vanishing wall distance can be described by $u'/u_\tau = 0{\cdot}28y^+ + Cy^{+3}$, where C is also a constant.

5.2. *Comparison of streamwise velocity fluctuations and velocity gradients at the wall*

Two completely identical sets of electronic equipment were used to simultaneously record the instantaneous values of the velocity gradient at the wall and the streamwise velocity fluctuations. The probes used for the preceding measurements were also used here. The hot film was aligned parallel to the wall and normal to the direction of the flow; the hot-film wall element also lay with its long axis normal to the direction of the flow. Both probes had the same x and z co-ordinates and were located 10 cm below the surface of the oil and 675 cm downstream from the screen, as before.

Figure 6 shows the simultaneously recorded measurements of the velocity gradient $(\partial u/\partial y)_0$ at the wall and the streamwise velocity fluctuations u as functions of time for 10 different distances from the wall and for $Re_U = 8200$. Since the shapes of the curves were to be compared, the vertical scale of the streamwise fluctuations for each distance from the wall was adjusted so that $(\partial u/\partial y)_0$ and u could be recorded with approximately the same amplitude. The records are arranged so that the $u(t)$ curves lie beneath the corresponding records of the wall gradient. As one can see, the $u(t)$ records for $y^+ \lesssim 7$ are very similar to the gradient records $(\partial u(t)/\partial y)_0$. The increasing lack of similarity between $u(t)$ and $(\partial u(t)/\partial y)_0$ with increasing distance from the wall is due to the appearance of higher frequencies in the streamwise fluctuations. These frequencies are superimposed on and increasingly determine the shape of these fluctuations as a function of time. The similarity of the $u(t)$ signals in the viscous sublayer at different y^+ positions reported by Gupta (1970) accords well with the present observations. Laufer's (1950) measurements of the spectral distribution of turbulent fluctuations near the wall show an increase in energy in the high frequency portion of the spectra with increasing distance from the wall, while the energy at low frequencies changes only slightly. This also agrees well with the trends shown in figure 6. The recorded signals have one very remarkable feature. The fluctuations $(\partial u(t)/\partial y)_0$ of the gradient at the wall lag behind the streamwise velocity fluctuations $u(t)$, with a lag time which increases with increasing distance of the hot-film probe from the wall. This means that an observed disturbance at a particular distance from the wall reaches the wall after some delay, or in other words, disturbances originating in the flow field move with a finite velocity towards the wall. The fact that the signal at the hot-film probe leads the signal at the wall element is to be expected from the visual data of Corino & Brodkey (1969) and Kline & Rundstadler (1959) and also from the hot-film measurements of Bakewell (1966). The observations of Corino & Brodkey suggest that the 'sweep' type motion, described as incoming high momentum fluid moving towards the wall at a slight angle, would be detected first by a probe in the flow before being detected at the wall. By means of dye injection, Kline

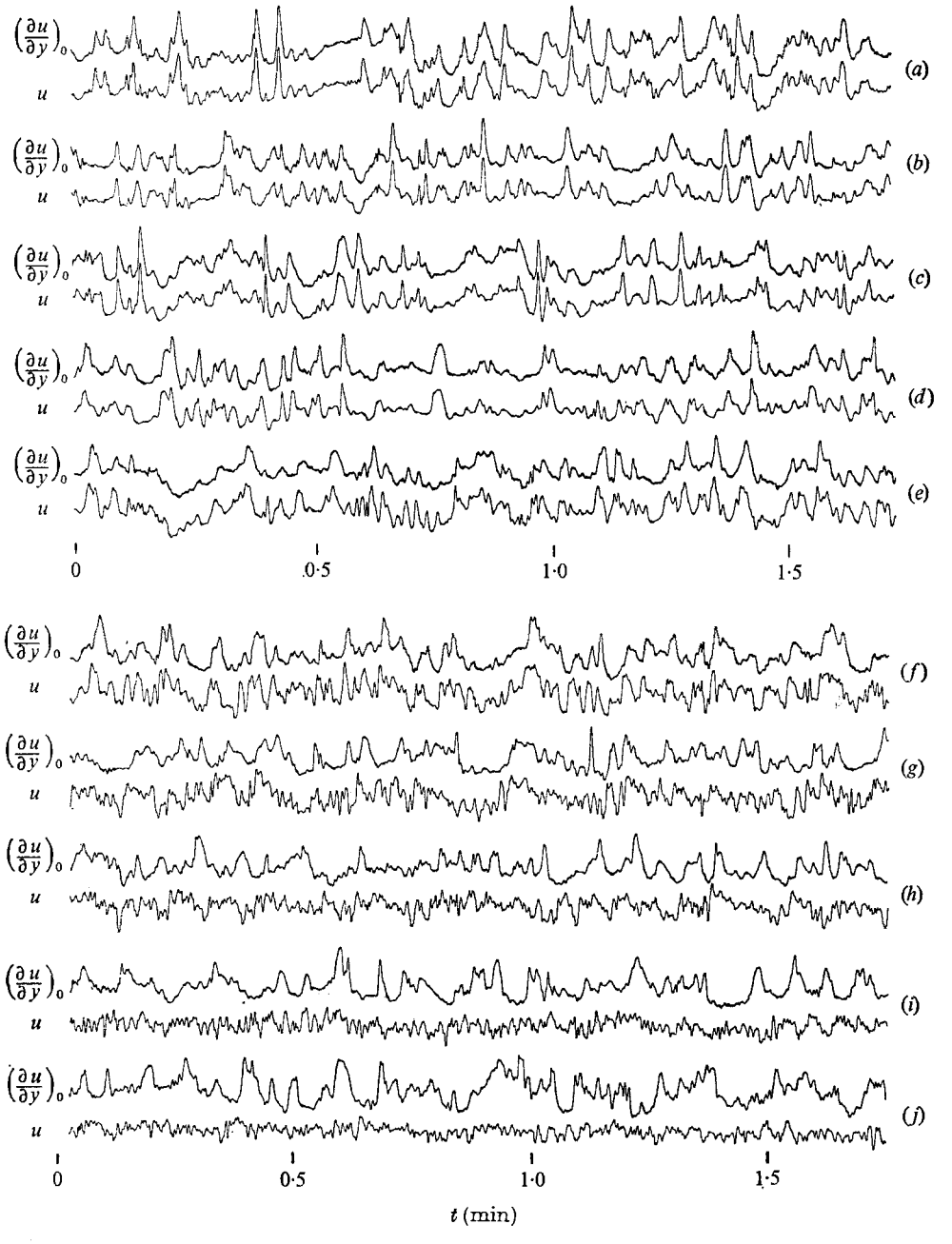

FIGURE 6. Simultaneous time records of instantaneous $(\partial u/\partial y)_0$ and fluctuations at various y^+ positions. $U = 22{\cdot}5$ cm/s, $Re_U = 8200$.

	(*a*)	(*b*)	(*c*)	(*d*)	(*e*)	(*f*)	(*g*)	(*h*)	(*i*)	(*j*)
y^+	1·0	1·9	2·9	4·8	8·6	12	25	36	58	114
y/b	0·005	0·009	0·014	0·023	0·041	0·06	0·12	0·17	0·27	0·55

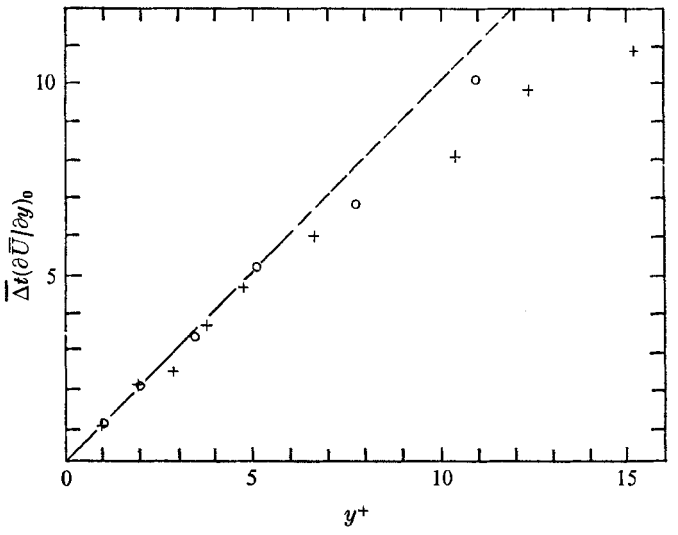

FIGURE 7. The lag time $\overline{\Delta t}$, non-dimensionalized by the mean value of the wall gradient, as a function of the non-dimensional wall distance y^+.

& Rundstadler observed that fluid at $y^+ \lesssim 0{\cdot}01$ lifts up while moving downstream. Such lifting fluid forms an inclined region which should pass a probe in the flow before affecting the probe at the wall. Bakewell's measurements also indicate that disturbances approach the wall at an inclination angle of about 8°. He explains this by the relatively diffuse flow towards the wall required by large eddy pairs.

In order to determine the propagation velocity normal to the wall of such disdisturbances, the lag times Δt were taken from the records. The results are shown in figure 7, where the mean values $\overline{\Delta t}$ of these lag times, made non-dimensional by multiplication by $(\partial\overline{U}/\partial y)_0$, are plotted against y^+. With this normalization, the values obtained for both Reynolds numbers fit a single curve when plotted against y^+. As one can see, the points up to $y^+ = 5$ lie practically on a straight line passing through zero with a slope of 1. Consequently, the lag time is approximately proportional to the distance from the wall; i.e. the propagation velocity $\bar{c}$ of the disturbances is nearly constant in this region. For $\bar{c} = y/\overline{\Delta t}$, it follows from $\overline{\Delta t}(\partial\overline{U}/\partial y)_0 \approx y^+$ that $\bar{c} \approx u_\tau$, since for $y^+ < 5$, $y^+ = \overline{U}/u_\tau$. Therefore, in figure 8, which shows $\bar{c}/u_\tau$ plotted against y^+, the points near the wall lie around a value of 1. This result is remarkable for two reasons. It is surprising that the propagation velocity is nearly constant for $0 < y^+ \leqslant 5$ and that this constant value corresponds to the friction velocity. A propagation velocity of $0{\cdot}8u_\tau$ can also be derived from Reichardt's (1971) theory on the viscous sublayer.

The cross-correlation of $(\partial u/\partial y)_0$ with u was also determined. Figure 9 shows the corresponding coefficient plotted against y^+ from the wall to the channel centre-line, for both Reynolds numbers. The slight decrease in correlation near the wall can be traced to the time lag of $(\partial u/\partial y)_0$ with respect to u. The sharp decrease in the coefficient at larger y^+ is due to the occurrence of higher frequency u fluctuations which are not correlated with the gradient fluctuations at the wall.

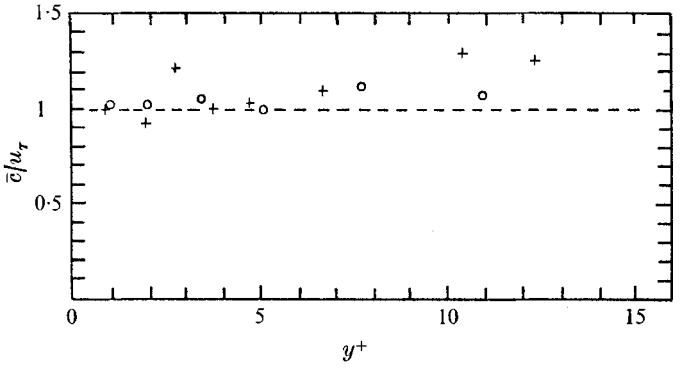

FIGURE 8. The normalized propagation velocity $\bar{c}$ as a function of the non-dimensional wall distance y^+.

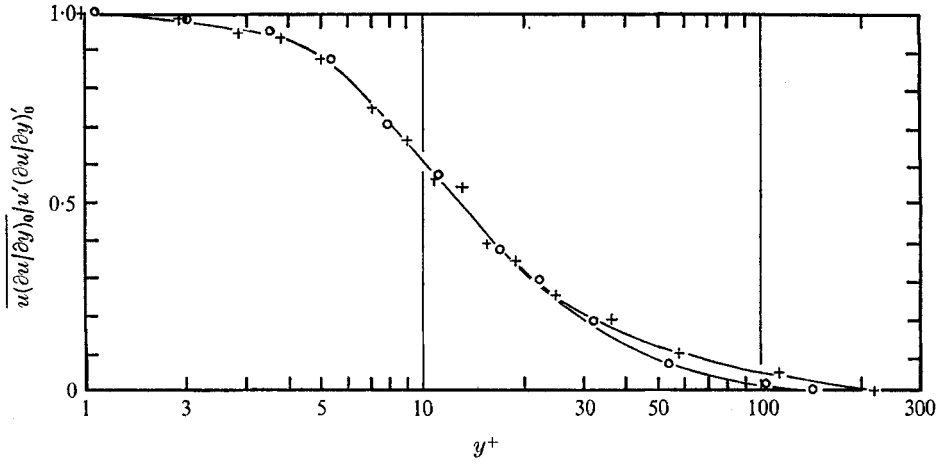

FIGURE 9. Correlation coefficient of u and $(\partial u/\partial y)_0$.

The correlation coefficient is 0·5 at $y^+ = 13$, where the maximum in u'/u_τ occurs. It should also be noted that the correlation coefficient is zero at the centre-line of the channel.

6. Probability density distributions of the streamwise velocity

The linearized hot-film signal of the single-film probe was connected to the LABEN analyser, digitized and sampled at each y^+ position every 10^{-3} s for 13 min. The analyser operates in the following manner. The digitized hot-film signal is sorted according to the voltage amplitude prevailing at that instant. Many meters, working in parallel but responding only to one fixed voltage interval, sum the number of digitized voltages which occur in that interval. By means of the calibration curve of the hot-film probe, each voltage interval can be related to a velocity interval. The number of observations which occur in each of the velocity intervals divided by the total number of occurrences (in

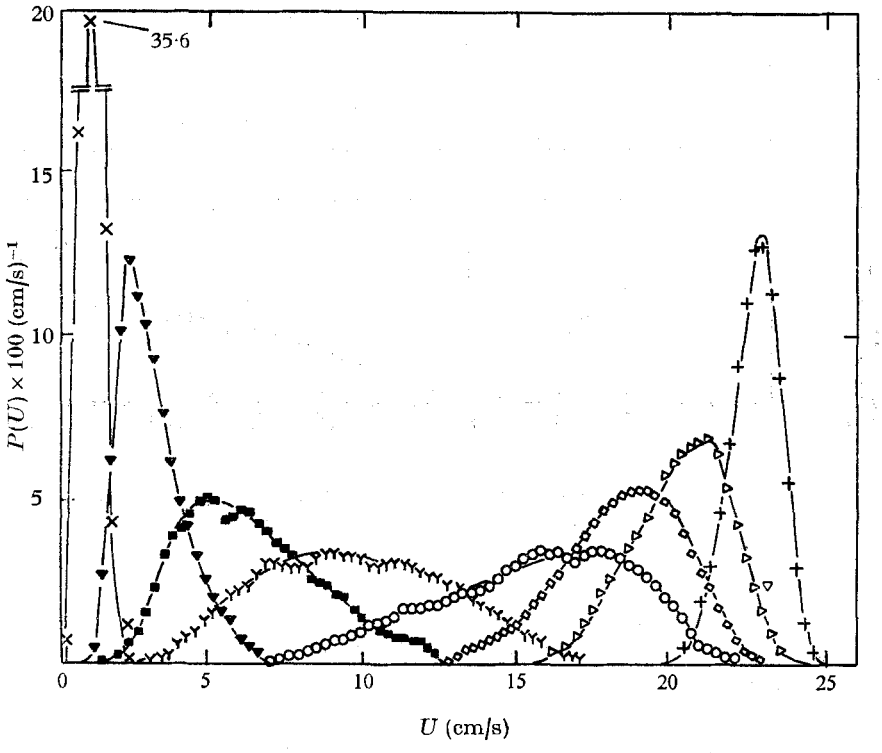

FIGURE 10. Probability density distribution of the instantaneous streamwise velocity at various y^+ positions. $Re_U = 8200$, $\overline{U}_c = 22{\cdot}5$ cm/s.

	×	▽	□	Y	○	◇	▷	+
y^+	0·8	2·7	5·1	8·0	19·0	38·0	76·0	210·0
y/b	0·004	0·013	0·025	0·038	0·090	0·180	0·360	1·000

this case 8×10^5) and by the interval width (in this case 0·28 cm/s) gives an estimate of the probability density distribution $P(U)$ of the streamwise velocity.

Figure 10 shows the probability density distributions for $Re_U = 8200$ so obtained. Since the probability density distributions for the smaller Reynolds number are very similar, they are not shown here. Recently Kreplin (1973) has been able to reproduce these results exactly with a top cover on the channel and the probe at the channel mid-depth. He also measured for the u fluctuations both the skewness factor $\overline{u^3}/(\overline{u^2})^{\frac{3}{2}}$ and the flatness factor $\overline{u^4}/(\overline{u^2})^2$ as functions of wall distance, and both factors for the gradient $(\partial u/\partial y)_0$ at the wall. Kreplin used a PDP 15 digital computer for his investigations. The linearization of the hot-film signals was done on-line using a fourth-order polynomial approximation. These results are shown in figure 11. Since the limiting probe values for the gradient at the wall cannot be displayed on this semi-log plot, the curves through the points have been drawn to indicate the values for $y^+ \to 0$. At the wall, the skewness factor has a value of 0·75 and the flatness factor a value of 3·7. A comparison of figures 10 and 11 shows that the largest streamwise velocity fluctuation amplitudes occur at $y^+ \approx 13$, as one would expect from the measurements of the

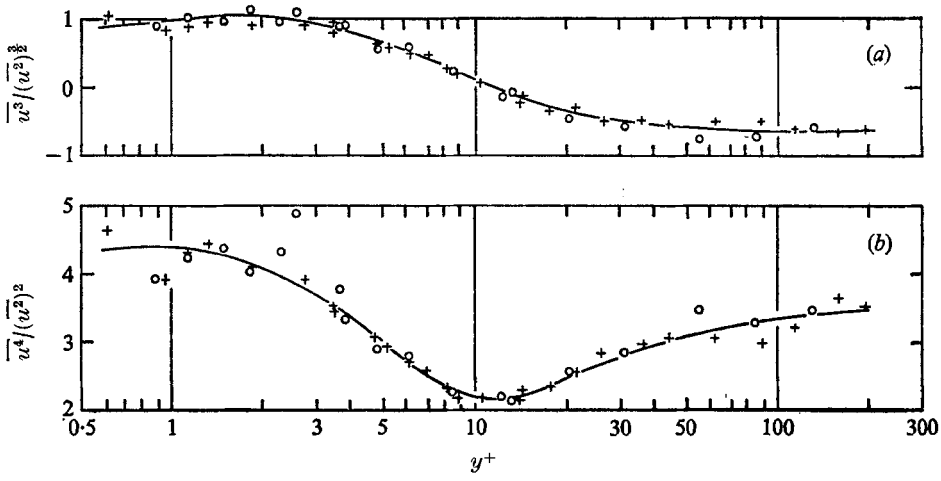

FIGURE 11. Distribution of (*a*) the skewness and (*b*) the flatness factors of the streamwise velocity fluctuations over the channel half-width, from Kreplin (1973). ○, $Re_U = 4800$; +, $Re_U = 7100$.

streamwise fluctuations shown in figure 5. The probability density distribution is symmetric only at this distance from the wall, but is not Gaussianly distributed. A Gaussian distribution has a flatness factor of 3·0 and is not skewed. At $y^+ \approx 13$, only the latter quality is fulfilled. At all other distances from the wall, the distributions are skewed, i.e. the mean and the most probable velocity do not coincide. At distances $y^+ < 13$, the most probable velocities are less than the local mean velocity; for $y^+ > 13$, the opposite is found. Even at the centre of the channel the distribution is asymmetric with the local mean velocity still smaller than the most probable velocity.

The distributions reported here are in good agreement with the work of Schraub & Kline (1965). They reported that low-speed streaks observed visually in the region $y^+ < 10$ are wider and high-speed streaks narrower. Since the location of these streaks is random, one must find, if the average is taken over a long enough time, that the most probable velocity is less than the mean velocity. For $y^+ > 10$, they found high-speed streaks to be wider and the low-speed streaks narrower, thus yielding the opposite skewness in this region. Hence, in the case of Schraub & Kline, a symmetric distribution would be expected for $y^+ = 10$, which agrees fairly well with the present results.

The skewness and flatness factors obtained by Kreplin check well in the logarithmic region of the velocity profile with the measurements made by Comte-Bellot (1965), and in the region $y^+ < 30$ with the results obtained by Gupta & Kaplan (1972).

Finally, the widths $\Delta u_{\frac{1}{2}}$ between the half-maximum values of the probability density distributions, non-dimensionalized with the friction velocity u_τ, are plotted *vs.* y^+ in figure 12 for both Reynolds numbers. The data collapse onto one curve, and again the maximum lies at $y^+ \approx 13$ as does the maximum of u' in figure 5.

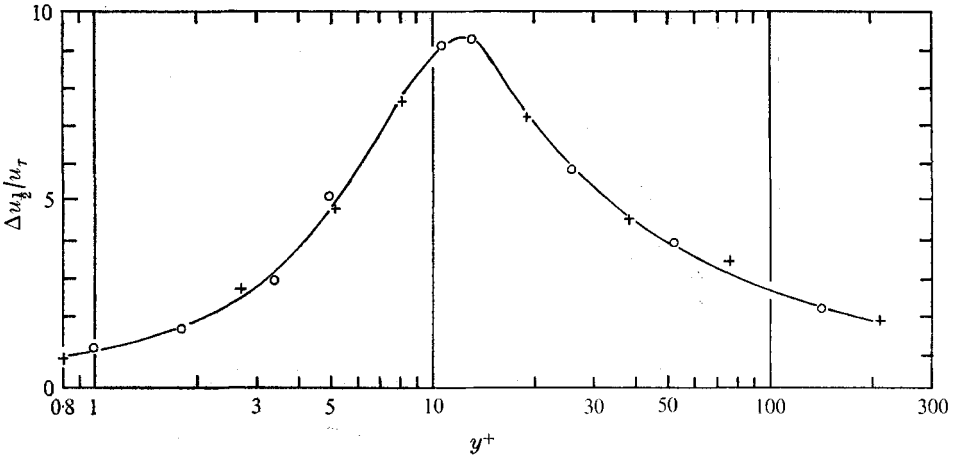

FIGURE 12. Width of the half-maximum values $\Delta u_{\frac{1}{2}}$ of the probability density distributions normalized with the friction velocity over the channel half-width.

7. The intermittent nature of the Reynolds stress

The TSI X-probe was used to measure the turbulent shear stress $-\rho\overline{uv}$ and to record the instantaneous uv signals. The width of the probe was 1·5 mm, since both films of the probe had to lie in the x, y plane. When non-dimensionalized with the wall parameters u_τ and ν, this width is $d^+ = 1{\cdot}9$ for $Re_U = 5600$ and $d^+ = 2{\cdot}8$ for $Re_U = 8200$. To operate both hot films and to process further their signals, two identical sets of electronics were again used. The voltage proportional to the velocity component $U = \overline{U} + u$ is obtained from the sum, and that proportional to v from the difference of the two linearized hot-film signals. Two Krohn–Hite filters were used; one was needed to obtain the streamwise fluctuating component u by filtering out the d.c. voltage corresponding to $\overline{U}$. The other filter was used for the transverse fluctuating component v and was necessary in order to compensate for phase errors possibly introduced by the first filter. Reliable measurements were only then possible when both sets of anemometers and linearizers were so balanced that the criterion $\Sigma v = 0$ was fulfilled for the duration of the measurements. The balancing was done individually for each y^+ position, and therefore a calibration was required for each point. The results obtained with this probe near the wall are shown in figure 13. The first plot shows the distribution of the normalized r.m.s. streamwise fluctuations u'/u_τ together with the measurements (solid line) already presented in figure 5. The normalized r.m.s. normal component v'/u_τ and the distribution of the normalized Reynolds stress $-\overline{uv}/u_\tau^2$ are shown in the centre and lower plots, respectively. The solid curve for $-\overline{uv}/u_\tau^2$ in the lower plot was obtained from the equations of motion for a turbulent channel flow (see Tennekes & Lumley 1972, equation 5.2.8). For comparison purposes, the probe dimension d^+ for both Reynolds numbers is also shown.

The intermittent nature of the instantaneous uv signals shown in figure 14 is apparent. In the records of the signals taken in the viscous sublayer ($y^+ = 2{\cdot}9$

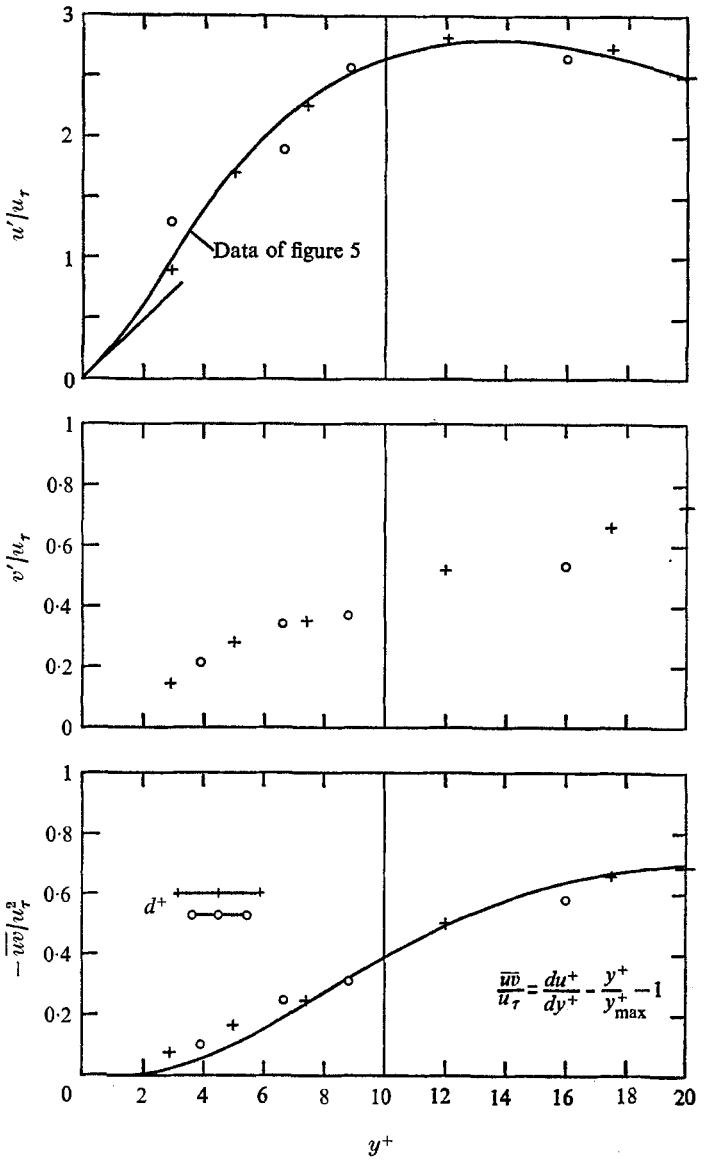

FIGURE 13. Distribution of u', v' and $-\overline{uv}$ in the vicinity of the wall, all normalized with the friction velocity. ○, $Re_U = 5600$; +, $Re_U = 8200$.

and 5·0), there are often periods of almost complete quiescence in the uv signals, although the highest turbulence level $u'/\overline{U}$ in the whole flow field (about 35–38 %) occurs here. In figure 14, the mean values $-\overline{uv}$ measured during the recording time are shown at the immediate left of the recorded signals. The mean values are rather small in comparison with the peaks; peak-to-mean ratios of 30:1 at $y^+ = 2{\cdot}9$ and 5·0 can be seen in these traces. At times even higher ratios could be observed. At the centre-line, positive and negative peaks are nearly equal in height. At positions closer to the wall, though, the negative peaks predominate

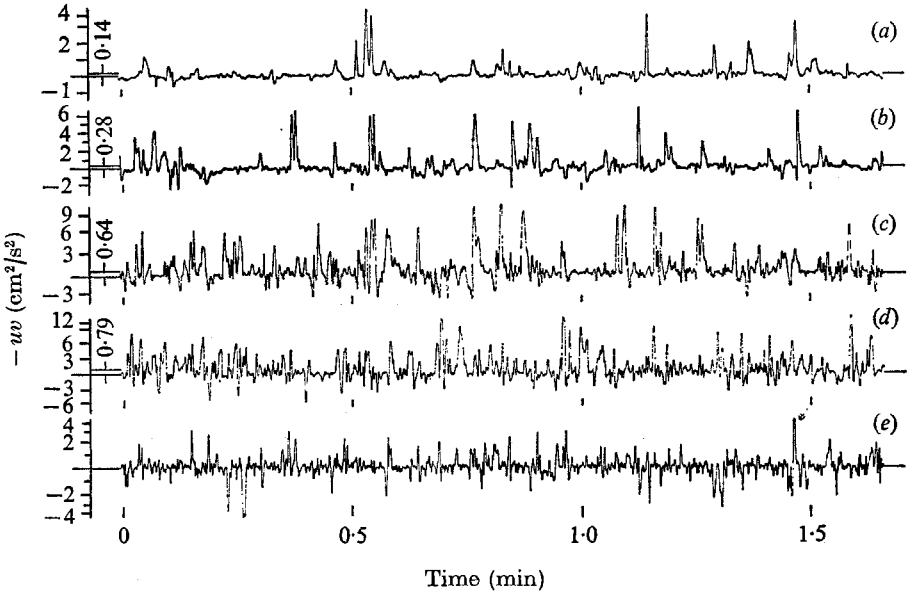

FIGURE 14. Instantaneous turbulent shear stress $-\rho uv$. $U = 22{\cdot}5$ cm/s, $Re_U = 8200$.

	(*a*)	(*b*)	(*c*)	(*d*)	(*e*)
y^+	2·9	5·0	12	20	210
y/b	0·014	0·024	0·057	0·098	1·000

somewhat over the positive ones, so that a relatively small mean value of $-\overline{uv}$ results. Throughout the whole log-law region of the turbulent flow, the picture of the instantaneous uv signal is similar to that represented by the fourth record from the top in figure 14. This is also expressed by the constancy of the correlation coefficient $-\overline{uv}/u'v'$ in this region, at about $-0{\cdot}4$ (Eckelmann 1970). The picture changes as the wall is approached, however. Here almost all peaks of $-uv < 0$ have died out, which is in agreement with the results of Wallace, Eckelmann & Brodkey (1972). In this region, the negative contributions to the Reynolds stress $-\overline{uv}$ of the interaction-type motions they observed ($u > 0, v > 0$ and $u < 0, v < 0$) approach zero.

The intermittent structure of the Reynolds stress in the wall region has been reported in the past by Corino & Brodkey (1969), Gupta (1970), Kim, Kline & Reynolds (1971), Wallace *et al.* (1972) and most recently, by Willmarth & Lu (1972). In this paper, however, a comparison of the time function $-uv(t)$ can be made over the full channel width.

8. Recapitulation and conclusion

(i) The temporally fluctuating velocity gradient at the wall is always positive (figure 4).

(ii) All the values of u'/u_τ measured at distances $y^+ > 0{\cdot}8$ lie above the straight line $u'/u_\tau = 0{\cdot}24y^+$ obtained with a hot-film wall element. In the immediate

vicinity of the wall ($y^+ < 0{\cdot}1$), the u fluctuations are nearly proportional to the distance from the wall and approach this line asymptotically with decreasing y^+ (figure 5). This indicates that a viscous wall layer exists under the sublayer ($0 \leqslant y^+ \lesssim 0{\cdot}1$), in which both the streamwise fluctuations u' and the mean velocity $\overline{U}$ vanish linearly with decreasing wall distance.

(iii) The time dependence of the u fluctuations in the wall layer $0 < y^+ < 12$ is very similar to that of the velocity gradient at the wall (figure 6). A time delay which is nearly proportional to y^+ accounts for the primary differences between these simultaneously recorded records. The large u fluctuations travel towards the wall with a nearly constant velocity $\bar{c}$. From the averaged time delays measured for the various distances from the wall, it was seen that the mean propagation velocity $\bar{c}$ almost corresponds to the friction velocity u_τ (figure 8).

(iv) The probability density distributions $P(U)$ of the instantaneous streamwise velocity are asymmetric on both sides of $y^+ \approx 13$. Close to the wall, $y^+ < 13$, velocities which are lower than the local mean value $\overline{U}$ occur most often. At distances $y^+ > 13$, the opposite is the case.

(v) Highly intermittent instantaneous values of the Reynolds stress in the vicinity of the wall, with peaks of more than 30 times the mean value, were observed.

I should like to thank Dr H. Reichardt for suggesting the topic of this investigation and Professor E.-A. Müller for his interest in this work. Herr H.-P. Kreplin provided me with the results shown in figure 11. I should like to thank Dr J. M. Wallace for help with some of the measurements and for various discussions and Herr E. Kunze, who originally constructed the oil channel. Ms C. Dufala aided in the translation, Frau Köneke typed the manuscript and Frau Wahle made the drawings.

REFERENCES

Bakewell, H. P. 1966 Ph.D. dissertation, Pennsylvania State University.

Comte-Bellot, G. 1965 *Publ. Sci. Tech. du Ministère de l'Air, Paris*, no. 419.

Corino, E. R. & Brodkey, R. S. 1969 *J. Fluid Mech.* **37**, 1.

Eckelmann, H. 1970 *Mitteilungen aus dem MPI für Strömungsforschung und der AVA Göttingen* (available in English).

Eckelmann, H. 1972 *DISA Inf.* **13**, 16.

Fortuna, G. & Hanratty, T. J. 1971 *Int. J. Heat Mass Transfer*, **14**, 1349.

Freymuth, P. 1967 *Rev. Sci. Instrum.* **38**, 677.

Gupta, A. K. 1970 Ph.D. dissertation, University of Southern California.

Gupta, A. K. & Kaplan, R. E. 1972 *Phys. Fluids*, **15**, 981.

Kim, H. T., Kline, S. J. & Reynolds, W. C. 1971 *J. Fluid Mech.* **50**, 133.

Klatt, F. 1973 *DISA Inf.* **14**, 25.

Kline, S. J. & Rundstadler, P. W. 1959 *J. Appl. Mech., Trans. A.S.M.E.* **26**, 166.

Kreplin, H.-P. 1973 *MPI für Strömungsforschung, Göttingen, Rep.* no. 2/1973.

Laufer, J. 1950 *N.A.C.A. Tech. Note*, no. 2123.

Laufer, J. 1954 *N.A.C.A. Tech. Rep.* no. 1174.

Obermeier, F. 1972 *MPI für Strömungsforschung, Göttingen, Rep.* no. 132/1972.

Popovich, A. T. & Hummel, R. L. 1967 *A.I.Ch.E. J.* **13**, 854.

PY, B. 1973 *Int. J. Heat Mass Transfer*, **16**, 129.

REICHARDT, H. 1938 *Naturwissenschaften*, **24/25**, 404.

REICHARDT, H. 1971 *MPI für Strömungsforschung, Göttingen, Rep.* no. 6a/1971 (in English).

SCHRAUB, F. A. & KLINE, S. J. 1965 *Thermosci. Div., Mech. Engng Dept., Stanford University, Rep.* MD-12.

TENNEKES, H. & LUMLEY, J. L. 1972 *A First Course in Turbulence.* M.I.T. Press.

WALLACE, J. M., ECKELMANN, H. & BRODKEY, R. S. 1972 *J. Fluid Mech.* **54**, 39.

WILLMARTH, W. W. & LU, S. S. 1972 *J. Fluid Mech.* **55**, 65.